



Article

Dielectric Properties and Energy Storage of Hybrid/Boron Nitride/Titanium Carbide/Epoxy Nanocomposites

Chryssanthi Blatsi, Anastasios C. Patsidis and Georgios C. Psarras *

Smart Materials & Nanodielectrics Laboratory, Department of Materials Science, School of Natural Sciences, University of Patras, 26504 Patras, Greece

* Correspondence: g.c.psarras@upatras.gr; Tel.: +30-261-0996-316

Abstract: In this study, hybrid boron nitride (BN)/titanium carbide (TiC)/epoxy resin composite nanodielectrics were manufactured and characterized. Their morphological and structural characterization was conducted via scanning electron microscopy (SEM) images and X-ray diffraction (XRD) patterns, whereas the dielectric behavior was studied by means of broadband dielectric spectroscopy (BDS). Dielectric measurements were carried out from 30 to 160 °C and from 10^{-1} to 10^6 Hz, respectively. The dielectric results revealed the existence of three relaxation mechanisms, which from high to low frequencies, at constant temperature, refer to re-arrangement of polar-side groups (β -relaxation) of the macromolecular chains, transition from glassy to rubbery state of the amorphous polymer matrix (α -relaxation) and interfacial polarization (IP) between the polymer matrix and the nanofillers. It was found that, in general, nanodielectrics exhibited enhanced dielectric properties mainly due to the high dielectric permittivity of TiC and the fine dispersion of the fillers, confirmed also by the SEM images. Dynamic analysis conducted for the α -relaxation showed a Vogel–Fulcher–Tammann dependence on temperature. The ability of energy storing of the nanocomposites was examined via their energy density. Optimum performance is exhibited by the 5 phr TiC/1 phr BN/epoxy nanocomposite, reaching an energy storing ability nine times greater than the unfilled matrix.

Keywords: hybrid nanocomposites; nanodielectrics; dielectric relaxations; electrical properties; energy storing



Citation: Blatsi, C.; Patsidis, A.C.; Psarras, G.C. Dielectric Properties and Energy Storage of Hybrid/Boron Nitride/Titanium Carbide/Epoxy Nanocomposites. *J. Compos. Sci.* **2022**, *6*, 259. <https://doi.org/10.3390/jcs6090259>

Academic Editor: Vincenza Brancato

Received: 28 July 2022

Accepted: 2 September 2022

Published: 7 September 2022

Publisher's Note: MDPI stays neutral with regard to jurisdictional claims in published maps and institutional affiliations.



Copyright: © 2022 by the authors. Licensee MDPI, Basel, Switzerland. This article is an open access article distributed under the terms and conditions of the Creative Commons Attribution (CC BY) license (<https://creativecommons.org/licenses/by/4.0/>).

1. Introduction

It is well-known that polymer nanocomposites concentrate, worldwide, an enhanced scientific and technological interest, because of their ability to combine the supplementary or diverging properties of the polymer matrix and the nanoreinforcing phase, mostly at low filler content. By these means, polymer nanocomposites exhibit a versatile performance, thus achieving increased functionality [1–5]. The successful selection of the constituent materials for the fabrication of nanocomposites could lead to the development of systems displaying properties and behavior “on demand”. Under a suitable stimulus or signal control nanocomposite systems could be able to demonstrate the desirable properties and performance at service [2–5]. Varying the type, the morphology and the content of the reinforcing phase or phases, the properties of the nanocomposites become adjustable. Nowadays, multifunctional performance is considered almost as a prerequisite asset for technical materials in high tech applications. Multifunctionality can be described as the combination of various desirable properties in a composite material, which will exhibit all required performances at service, responding to different loading conditions and stimuli. This type of material should be characterized, among other aspects, by mechanical durability, thermal stability, adjustable dielectric behavior and conductivity, induced magnetic properties, suitable optical properties etc. Multifunctional performance can be further enhanced by employing, as a reinforcing phase, materials undergoing thermally or electrically triggered phase changes and by developing composite systems where electrical

energy can be stored and sufficiently retrieved [6–8]. The latter could be achieved in many nanocomposites, since the dispersed nanoinclusions can act as a distributed network of nanocapacitors [9]. Furthermore, hybrid nanocomposites employing two reinforcing phases could be able to exploit in their performance selected properties from all three constituents [5].

As nanodielectrics are classified ceramic dielectrics with grain size at the nano level, or polymer matrix composites with nanoinclusions [9]. Current applications of polymer nanocomposites include, although are not limited, electronic devices, electric vehicles, cellular phones, stationary power systems, wireless personal digital assistants, self-current regulators, integrated capacitors, conductive adhesives, acoustic emission sensors, memory switches and cases for electromagnetic shielding, as well as applications in the automobile, aerospace, and sports industries.

Epoxy resins are by far the most popular matrices in composites materials, because of their resistance to chemical attacks and corrosive environments, their thermal stability and mechanical sustainability, their low shrinkage and moisture absorbance, in tandem with the easy manufacturing procedure, the good adhesion with many fillers and their low cost [10,11].

Nowadays, 2D inclusions, like boron nitride (BN), have attracted huge interest. BN is a honeycomb-sheet with one atom thickness, high specific area and high Young's modulus. The smooth surface without any charge traps, the low dielectric constant and high-temperature stability and thermal conductivity of BN makes it suitable to act as a regulator in a composite system tailoring its electrical properties [12,13]. The geometrical configuration of BN and its morphology, increases the surface–volume ratio and allows the polymer matrix to adhere better to the nanosheets. Moreover, the atoms' configuration in the BN sheets resemble that of graphene, and thus BN appears as a very promising 2D reinforcing material in nanodielectrics. Titanium carbide (TiC) is an engineering material characterized by high melting point, hardness, elastic modulus, electrical conductivity, and low coefficient of thermal expansion [14]. In the past polymer composites with TiC particles have been considered as a new type of smart materials since they have been found to change the sign of the temperature coefficient of conductivity from positive to negative and vice versa [15–18]. In the present study, it is attempted for the first time, to combine the reinforcing abilities of the spherical-like nanoparticles of TiC with the 2D BN by fabricating hybrid nanocomposites with an epoxy resin as matrix. Upon fabrication and morphological/structural characterization, the electrical properties of nanocomposites and their ability to store electrical energy is investigated. Finally, interactions occurring between the constituents of the hybrid nanocomposites and their synergy is discussed.

2. Materials and Methods

For the fabrication of the nanocomposites a liquid epoxy resin (Epoxol 2004 A) prepolymer and a slow-rate curing agent (Epoxol 2004 B) obtained from Neotex S. A., Greece, were employed as the polymer matrix. The reinforcing nanopowders were titanium carbide (TiC) and hexagonal boron nitride (h-BN), purchased from Sigma Aldrich and Thomas Swan & Co. Ltd., respectively. Titanium carbide powder was in the form of nanoparticles with a diameter less than 200 nm, as noted by the supplier's datasheet. Hexagonal boron nitride powder consists of 2D platelets with high aspect ratio (>200) and lateral size less than 1 μm .

The fabrication process began by mixing precalculated amounts of h-BN and TiC nanopowders with the prepolymer of resin. The resulting mixture was stirred under ultrasonication, for 10 min at 50 °C. This procedure is important in achieving homogenous filler dispersion and in avoiding particles' agglomeration. The mixture was left to reach ambient temperature and then the curing agent was added to the mixture at a ratio 2:1 per weight resin/hardener. The resulted mixture was stirred very slowly for 15 min at room temperature and then poured into the molds. Curing took place at room temperature for a week, followed by a post-curing at 100 °C for 4 h. The whole fabrication process is

schematically shown in Figure 1. Filler content is expressed in part per hundred resin per mass (phr).

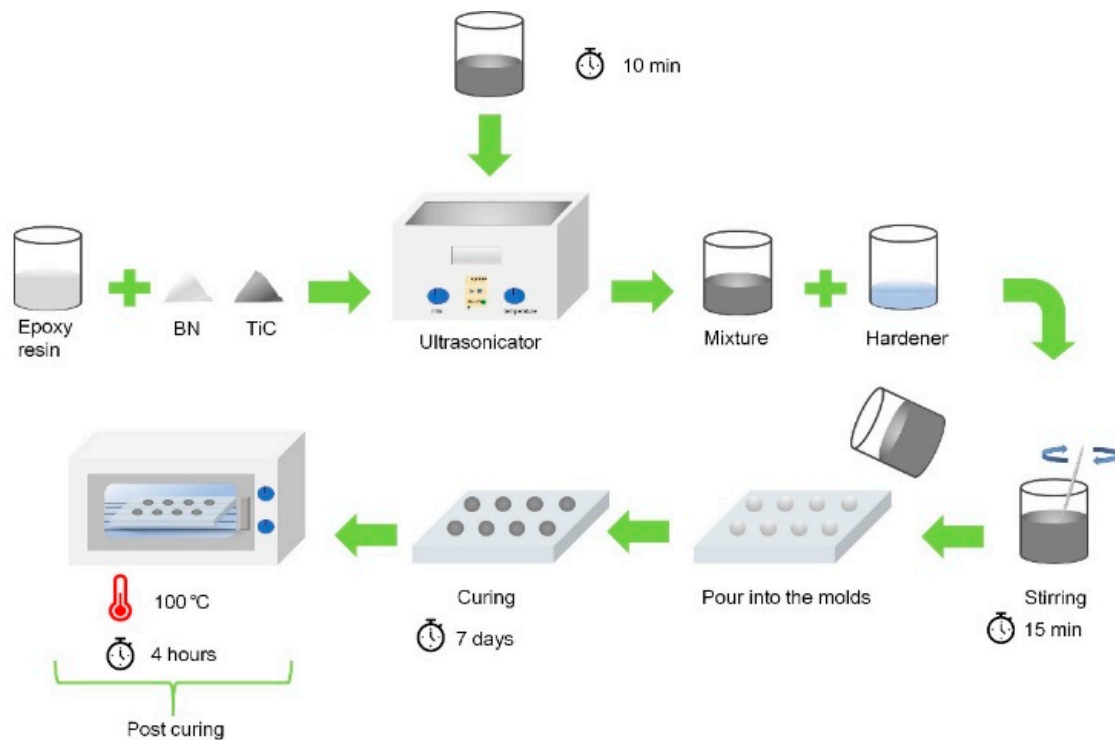


Figure 1. Schematic representation of the nanocomposites' fabrication procedure.

X-ray Diffraction (XRD) patterns were taken by means of a D8 Advance (Bruker AXS) device, using a Cu–K α source (1.54 Ångstrom, 1.6 kW) with scanning speed 0.5 s/step in the range of 20–90°. The dispersion of the fillers, as well as the existence of agglomerates and voids inside the nanocomposites, was examined using a Zeiss EVO-MA10 (Carl Zeiss Microscopy GmbH, Jena, Germany) Scanning Electron Microscope (SEM).

The dielectric characterization of the composites was conducted by means of Broad-band Dielectric Spectroscopy (BDS) with an Alpha-N Frequency Response Analyzer, supplied by Novocontrol Technologies (Hundsagen, Germany). Temperature was controlled via Novotherm system (Novocontrol Technologies) and the employed dielectric cell was BDS1200 (Novocontrol Technologies) with two parallel gold-plated electrodes. The measurements were carried out in the frequency and temperature range from 0.1 Hz to 10⁶ Hz and 30 °C to 160 °C, respectively. Frequency scans were conducted at constant temperature, with a step of 5 °C. Data acquisition, as well as frequency and temperature control were performed via windeta software (Novocontrol Technologies) at real time. The whole experimental procedure was in accordance with the ASTM D150 specification.

3. Results

3.1. Morphological and Structural Characterization of TiC/h-BN/Epoxy Systems

Scanning electron microscopy was used to study the morphology of each composite. The structural characterization was conducted by means of XRD patterns. Representative SEM images are depicted in Figure 2, where a fine and homogenous dispersion of the nanofillers in the polymer matrix is observed. In the systems with high nanoparticles content among nanodispersion, small and limited clusters can be detected. Figure 3 depicts the XRD patterns of BN and TiC powders, as well as the XRD diffractographs of TiC/BN/epoxy nanocomposites with different filler concentrations. The XRD pattern of BN powder implies its hexagonal crystalline structure due to the well-formed characteristic diffraction peaks at 26, 41, 50, 54 and 75 2 θ degrees, corresponding to the (002), (100), (102), (004) and (112) planes [19,20]. The TiC powder XRD pattern shows three very clear

peaks at 36, 41 and 60 2θ degrees, corresponding to the (111), (200) and (220) planes [21]. The XRD graph of the amorphous polymer matrix does not include any diffraction peaks. Hence, all the recorded peaks in the patterns of the nanocomposites correspond to the BN and TiC nanofillers and verify the successful integration of the nanoparticles in the epoxy resin. Moreover, the intensity of the peaks increases with filler concentration, meaning the successful nanocomposites' fabrication.

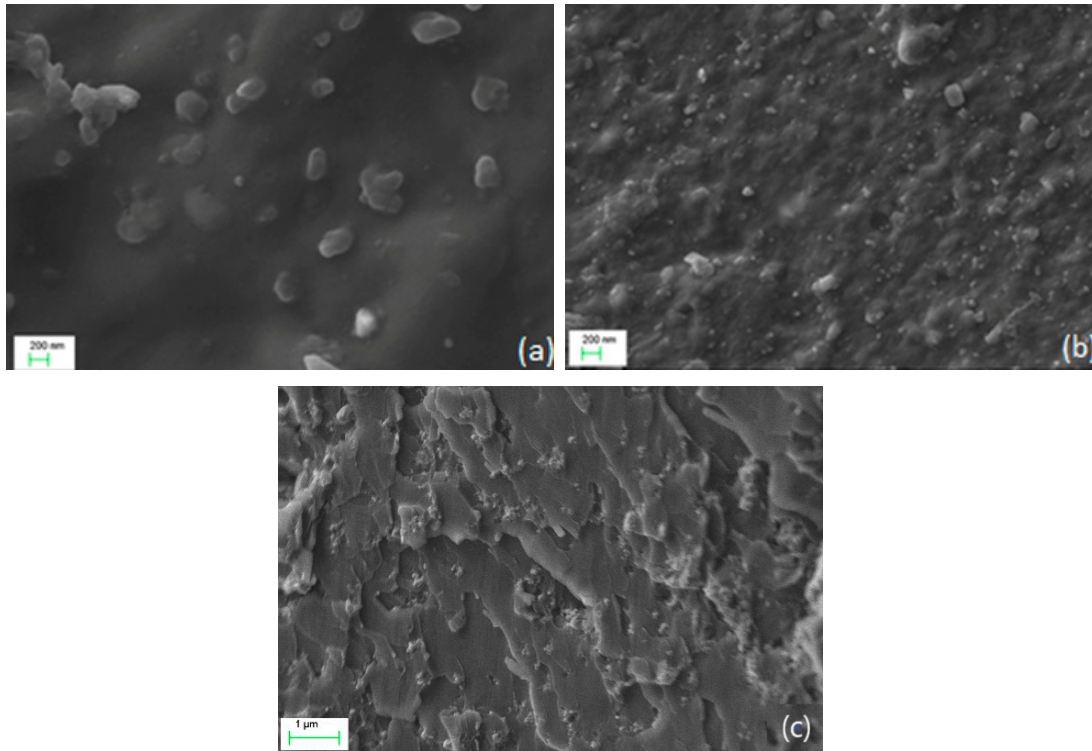


Figure 2. Representative SEM images of the: (a) 3 phr TiC/3 phr BN/epoxy, (b) 5 phr TiC/5 phr BN/epoxy and (c) 3 phr TiC/3 phr BN/epoxy (at a lower magnification) nanocomposites.

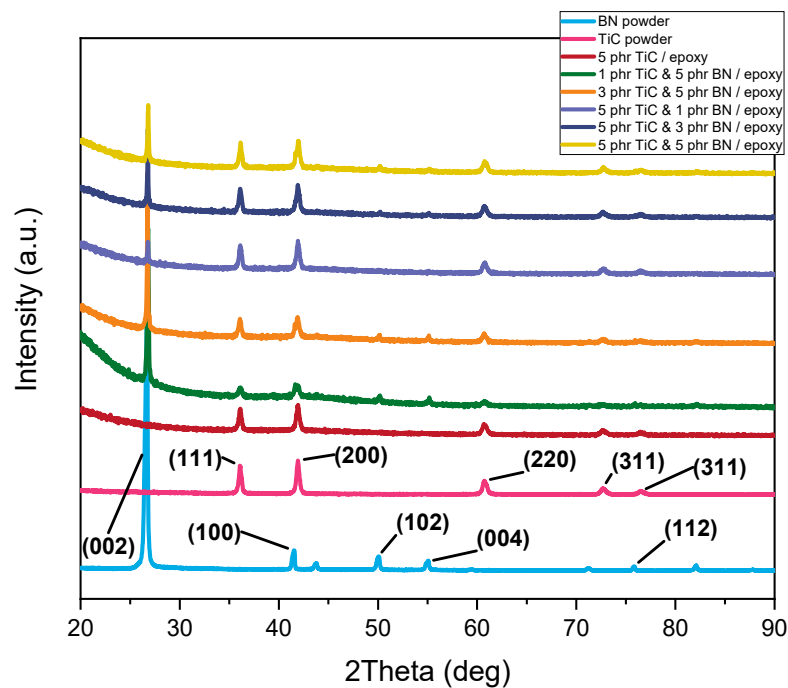


Figure 3. XRD patterns of studied hybrid composites and the employed fillers at room temperature.

3.2. Dielectric Response of TiC/h-BN/Epoxy Systems

Polymer matrix nanocomposites are mainly electrical insulators due to their low concentration of free charge carriers. Thus, they're electrically characterized by the relaxation phenomena that take place under AC field. These relaxations concern the orientation of both permanent and induced dipoles. The addition of nanofillers to the polymer matrix affects these relaxations and thus it is crucial to examine the influence of the nanofillers upon these relaxations. Obtained dielectric data are presented in the formalisms of dielectric permittivity, electric modulus, and AC conductivity. Figure 4a shows the 3D graph of the real part of the dielectric permittivity (ϵ') as a function of temperature and frequency for neat epoxy resin. In comparison, Figure 4b presents the corresponding data for the nanocomposite reinforced with 5 phr TiC/5 phr BN. In both cases, ϵ' attains high values at low frequencies and high temperatures, because sufficient time and thermal agitation is given to dipoles in order to be aligned with the applied field. The increase of the frequency of the applied field causes a rapid decrease of dielectric permittivity, since the fast alternation of the field results in diminishing of polarization. The reinforced specimen in Figure 4b exhibit higher values of ϵ' with respect to the epoxy sample because of the presence of the nanofillers. The same behavior, concerning ϵ' , was observed for the other systems, as well.

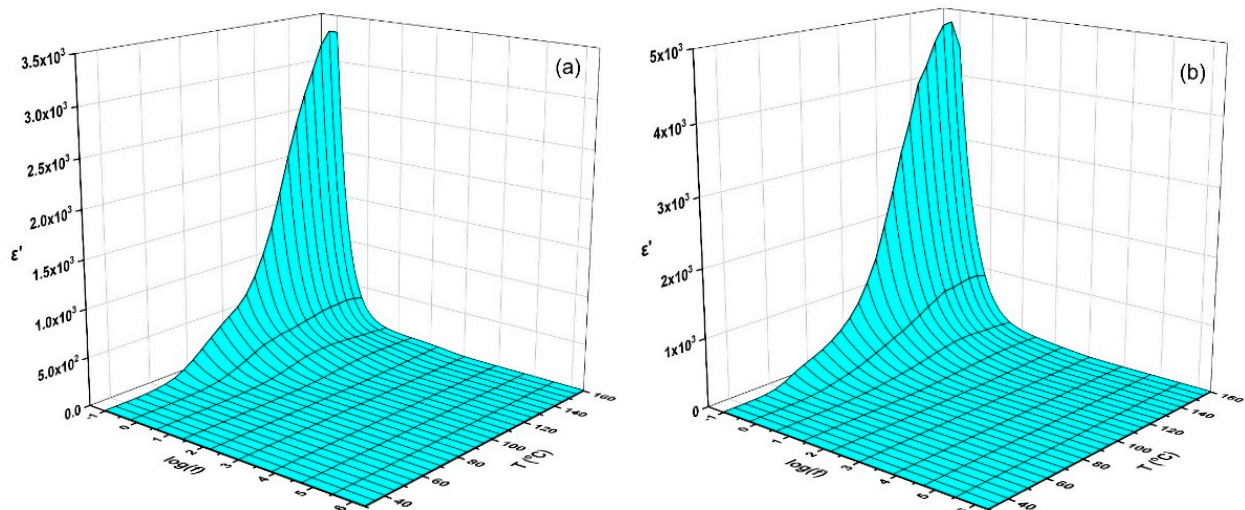


Figure 4. Real part of dielectric permittivity as function of frequency and temperature for: (a) unfilled epoxy and (b) 5 phr TiC/5 phr BN/epoxy nanocomposite.

Figure 5a,b depicts the 3D graphs of the loss tangent (δ) vs. temperature and frequency for the unfilled epoxy and the 5 phr TiC/5 phr BN/epoxy nanocomposite, respectively. The presence of relaxation processes becomes evident via the formation of peaks and humps. The weaker and faster relaxation (shorter relaxation time) is recorded in the high frequency range and is denoted as β -relaxation. This process is attributed to the movement/re-orientation of polar side groups of the polymer chain. At intermediate frequencies and temperatures, the glass to rubber transition occurs. The process is known as α -relaxation, is related to the amorphous polymer matrix, and is associated with the synergetic rearrangement of extensive parts of the main polymer chains. α -relaxation is a rather slow process. The loss $\tan\delta$ spectra of the unreinforced epoxy form a peak for α -relaxation, the position of which shifts to higher frequencies with the increase of temperature. Interestingly, the corresponding spectra for the 5 phr TiC/5 phr BN/epoxy nanocomposite depict a peak, for the same process, covering a broader frequency and temperature range. This peak appears to be formed by expanding, or even splitting, the peak of α -relaxation, of neat epoxy, into two parts and then shifting one part to higher and the other part to lower temperatures. This peak's widening is an indication for diverging interactions between the polymer matrix and the employed two different fillers. In general, strong interactions between macromolecules and nanoinclusions shift the glass to rubber transition peak to

higher temperatures, while weak interactions and possible low wettability of nanoparticles by the matrix shift the process to lower temperatures [22–24]. Finally, at low frequencies and high temperatures interfacial polarization (IP) takes place, due to the accumulation of electrical charges at the interface between the phases of the nanocomposite, where they form large dipoles at the surface around of the nanoinclusions. These induced dipoles attempt to follow the alternation of the field, but their inertia obstructs their orientation. At low frequencies sufficient time is given for their alignment, which is further facilitated by the thermal agitation [22,25].

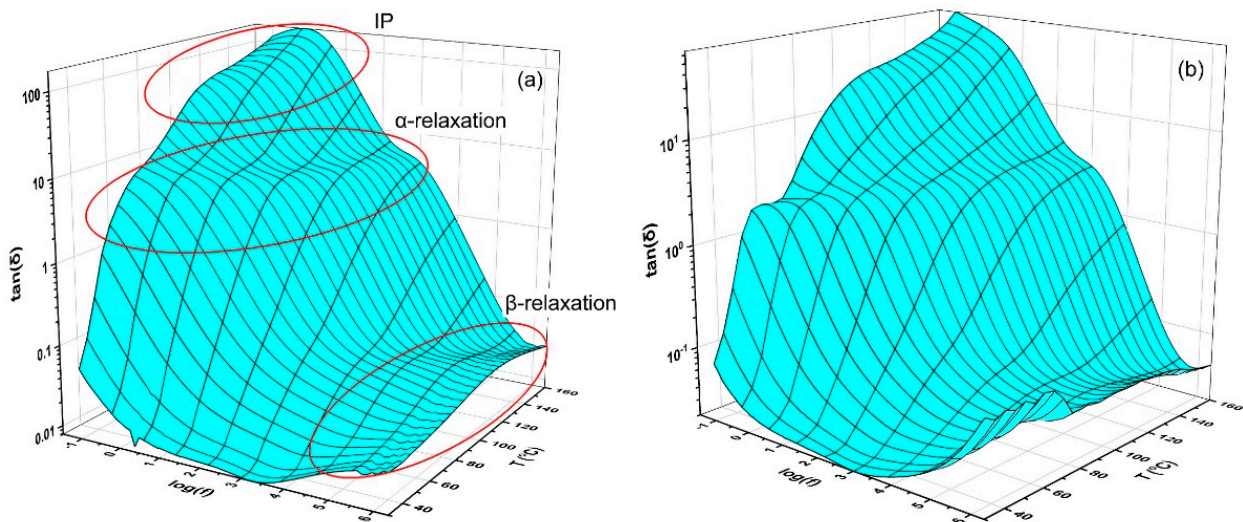


Figure 5. Loss $\tan\delta$ as function of frequency and temperature for: (a) unfilled epoxy and (b) 5 phr TiC/5 phr BN/epoxy nanocomposite.

The variation of AC conductivity as a function of frequency and temperature, for the unfilled epoxy and for the 5 phr TiC/5 phr BN/epoxy system, is shown in Figure 6a,b. Frequency-dependent conductivity has been determined according to Equation (1):

$$\sigma_{ac}(\omega) = \epsilon_0 \omega \epsilon'' \tag{1}$$

where ϵ_0 is the permittivity of vacuum, ω the angular frequency of the field, and ϵ'' the imaginary part of dielectric permittivity or loss index. Spectra of AC conductivity vary significantly with frequency and temperature over a range of six or seven orders of magnitude. In the low-frequency range, σ_{ac} tends to its DC value, while after a critical frequency an exponential dependence of AC conductivity upon frequency occurs. Effect of temperature upon the conductivity values is more pronounced in the low-frequency range. In the low-frequency edge, a limited number of charge carriers, migrate upon relative long distances. On the contrary, at high frequencies, an increased number of carriers moves forward/backwards between adjacent sites. By these means, “jumping” carriers contribute to the overall AC conductivity, although their spatial migration is very short. The spectra of Figure 6 are indicative for the examined systems, and in all cases σ_{ac} is in accordance with the AC universality law [26–28], as expressed by Equation (2):

$$\sigma_{ac}(\omega) = \sigma_{dc} + A\omega^s \tag{2}$$

where σ_{dc} corresponds to the DC value of conductivity and A, s are parameters depending on the temperature and the material [29]. The form of the recorded spectra of AC conductivity is considered as characteristic for charge transfer via hopping conductance [27,28].

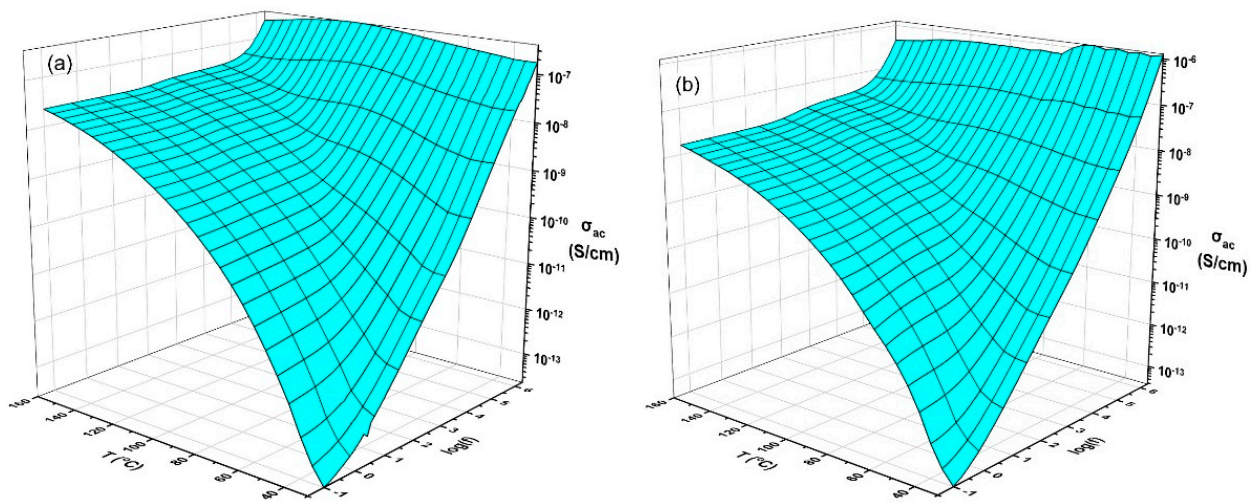


Figure 6. ac conductivity as function of frequency and temperature for: (a) unfilled epoxy and (b) 5 phr TiC/5 phr BN/epoxy nanocomposite.

4. Discussion

The electrical properties of the hybrid nanocomposites are determined to a great extent by the concentrations of the TiC and BN nanoinclusions. Figure 7 shows three comparative plots of ϵ' versus frequency or temperature, where the concentration of one filler type is kept constant and the second one gradually increases and vice versa. Figure 7a presents the variation of the real part of dielectric permittivity as a function of frequency, at 30 °C for the hybrids with constant TiC content at 5 phr and varying BN content. Nanocomposites exhibit higher values of ϵ' , than unfilled epoxy, in the whole frequency range. The dielectric reinforcing ability of TiC becomes evident, while at the same time a rather poor dielectric performance of BN is indicated. An analogous behavior is shown in Figure 7b, where the ϵ' , for the same systems, is plotted as a function of temperature at 1 kHz. Thermal agitation is beneficial to the orientation of dipoles and thus the real part of dielectric permittivity increases with temperature, denoting the enhancement of polarization. Besides the effect of fillers' loading, interfacial polarization at high temperatures increases further the values of ϵ' . The variation of ϵ' versus temperature, at 1 kHz, for nanocomposites with constant BN content at 5 phr and varying the TiC content is depicted in Figure 7c. Again, the presence of TiC augments the permittivity values, although the high content of BN restricts this alteration. Interestingly, in a previous study from our group concerning binary BN/epoxy nanocomposites [30], the effect of filler resulted in increased values of permittivity under the same testing conditions. The occurring interactions in the examined hybrids should be: (i) macromolecules-TiC particles, (ii) macromolecules-BN particles, and (iii) TiC particles-BN particles. Regarding these interactions and the recorded dielectric behavior, it can be suggested that the interactions between the two fillers induce the peculiarity of diminishing ϵ' with BN content.

Relaxation processes in polymeric systems can be studied via various formalisms, including electric modulus. Electric modulus is defined via Equation (3):

$$M^* = \frac{1}{\epsilon^*} = \frac{\epsilon'}{\epsilon'^2 + \epsilon''^2} + i \frac{\epsilon''}{\epsilon'^2 + \epsilon''^2} = M' + iM'' \tag{3}$$

where ϵ' , ϵ'' and M' , M'' are the real and imaginary parts of dielectric permittivity and electric modulus respectively. Electric modulus provides benefits in studying dielectric processes by neglecting electrode polarization [31–33].

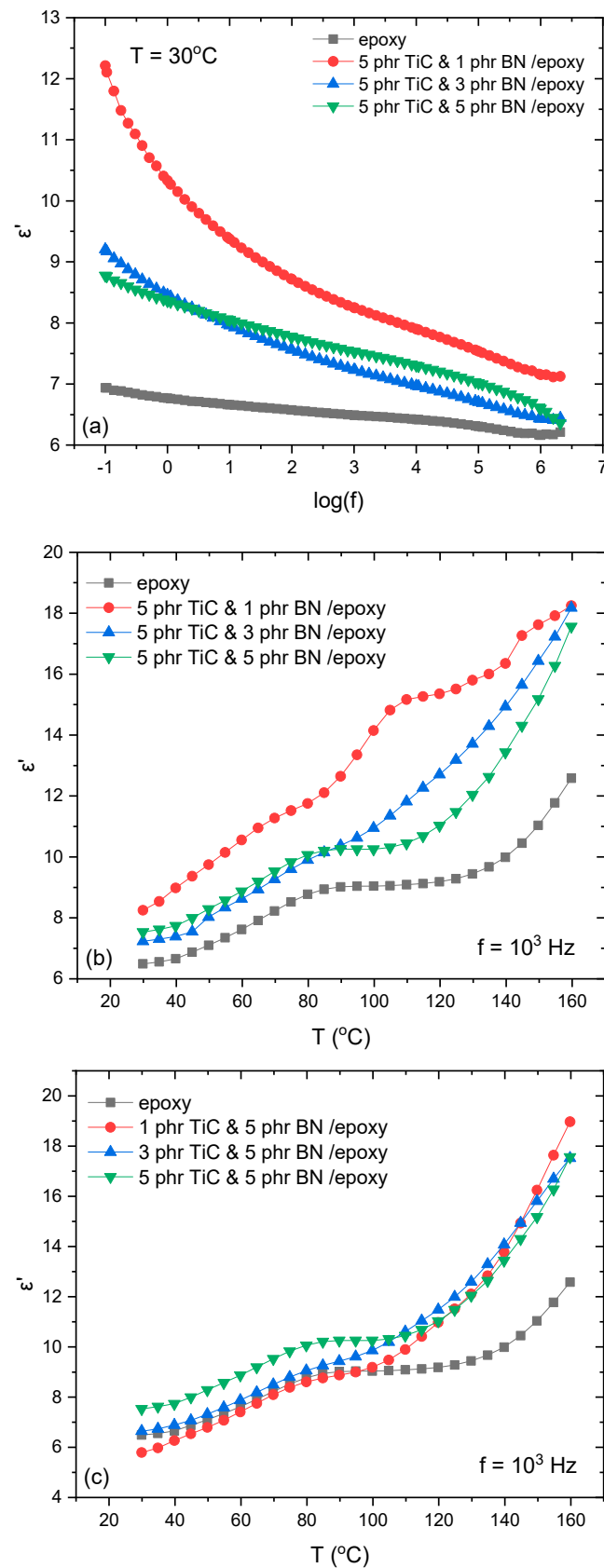


Figure 7. Real part of dielectric permittivity as a function: (a) of frequency, at 30°C , for the systems with 5 phr TiC, varying the BN content, (b) of temperature, at 1 kHz, for the same systems as in (a), and (c) of temperature, at 1 kHz, for the systems with 5 phr BN varying the TiC content.

The peak of α -relaxation versus temperature, at 1 kHz, is shown in the $M'' = f(T)$ plots of Figure 8a,b, with parameters the fillers content. When TiC content is kept constant at 3 phr, Figure 8a, varying BN content, the peak of the glass to rubber transition slightly shifts to lower temperatures, indicating a small decrease of T_g . An analogous behavior is detected in Figure 8b, where BN content is constant at 3 phr and concentration of TiC varies. Both cases imply the presence of moderate interactions between inclusions and macromolecules, since at strong or weak interactions T_g should be significantly increasing or decreasing, respectively [22,23,34]. However, the occurring synergy, or in other words the mutual interactions, between the two employed fillers is not easy to be examined and further research should be carried out. The presence of the 2D inclusions possibly exert spatial obstructions to molecular parts to be aligned with the applied field, leading by these means to the reduction of the real part of dielectric permittivity with BN content [35]. In addition, the 0D spheroid TiC nanoparticles increase ϵ' because of the augmentation of interfacial area and their enhanced conductivity, which increases the systems' heterogeneity. Spheroid nanoparticles could also act as a "bridging" medium between adjacent BN sheets, resulting in complex geometry of interfacial area and interfacial polarization.

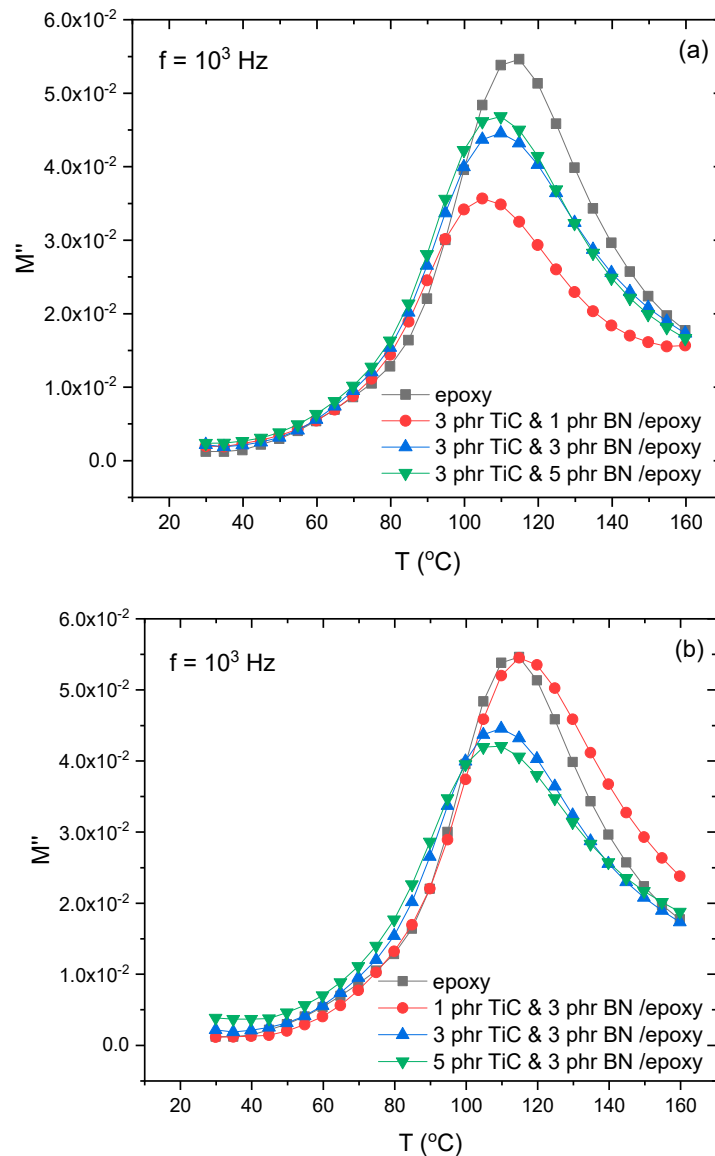


Figure 8. Imaginary part of electric modulus as a function of temperature, at 1 kHz, for the systems with: (a) 3 phr TiC, varying the BN content and (b) 3 phr BN, varying the TiC content.

Relaxation dynamics for the α -process are shown in Figure 9 for all studied systems. As expected, glass to rubber transition process follows a Vogel–Fulcher–Tammann (VFT) relation, for the frequency of the loss peak as a function of inverse temperature, Equation (4):

$$f_{max} = f_0 \exp \left[-\frac{B}{T - T_0} \right] \tag{4}$$

where f_0 is a pre-exponential factor, B is a parameter considered as a measure of activation energy, and T_0 is the Vogel temperature or ideal glass transition, which lies between 30 K and 70 K below the experimentally found T_g value [24,36].

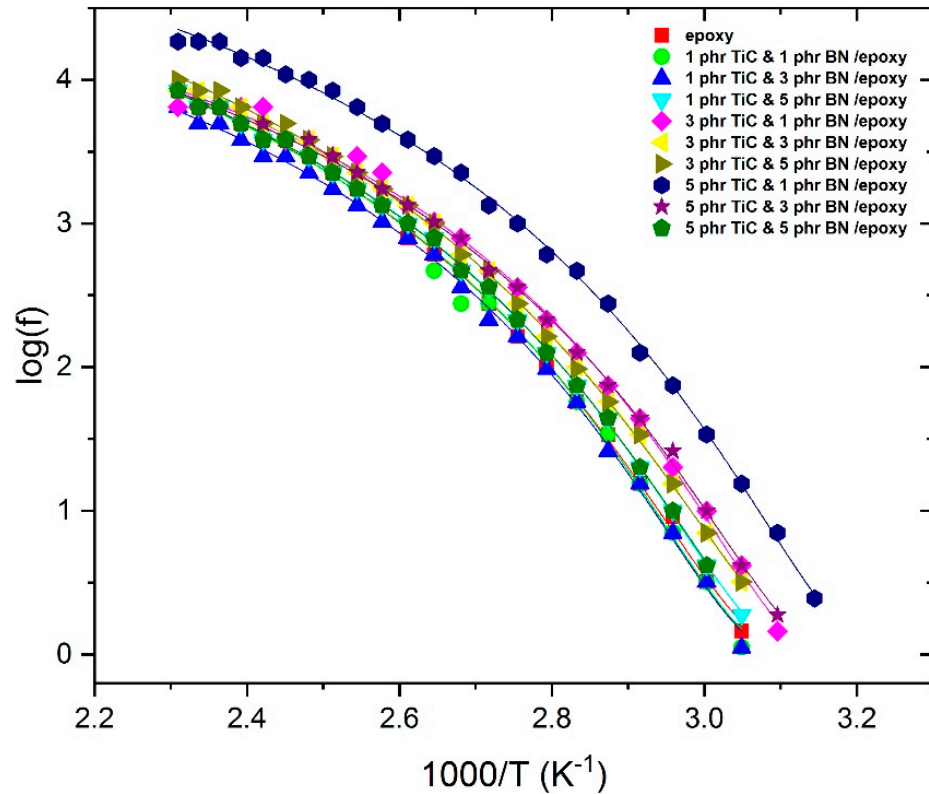


Figure 9. Dielectric loss peak position for α -relaxation, as a function of reciprocal temperature for all studied systems.

Table 1 summarizes the fitting parameters for all specimens. Recorded data didn't allow us to conduct a reliable fitting for the other two processes (IP and β -relaxation) and thus their dynamics is not presented.

Polymer matrix nanocomposites are systems where electric energy can be stored. The presence of nanoinclusions acts as a distributed network of nanocapacitors, which can be charged and discharged. Moreover, interfacial area and insulating matrix are also contributing to energy storing [6,37,38]. The ability of storing energy is expressed by energy density, which is defined according to Equation (5):

$$U = \frac{1}{2} \epsilon_0 \epsilon' E^2 \tag{5}$$

where ϵ_0 is the permittivity of vacuum, ϵ' the real part of dielectric permittivity of the material and E the intensity of the applied field. As it can be noted the only material parameter in Equation (5) is ϵ' , and thus the influence of the employed material on the energy density is expressed solely via the real part of dielectric permittivity. Energy density increases with the applied field and the dielectric breakdown strength sets the upper limit of its value. Figure 10a depicts energy density versus temperature, at 0.1 Hz, varying the

fillers' content, at $E = 1 \text{ kV/m}$. Energy density follows the dependence of ϵ' upon frequency, temperature and filler content. As it is depicted in Figure 10a, energy density increases significantly in the low-frequency and high-temperature region, where the effect of filler content becomes prominent because of interfacial polarization. Relative energy density defined via Equation (6), expresses the strengthening ability of filler content in comparison to unreinforced matrix:

$$U_{rel} = \frac{U_{comp}}{U_{matr}} \tag{6}$$

where U_{comp} and U_{matr} are the energy densities of the composite and the matrix at the same frequency, temperature, and applied field.

Table 1. Parameters obtained by fitting data for α -relaxation via Equation (4) for all studied systems.

Sample	T_0 (K)	B (K)	R^2
epoxy	313.6 ± 0.5	46.5 ± 0.4	0.998
1 phr TiC & 1 phr BN/epoxy	315.4 ± 0.4	44.2 ± 0.3	0.997
1 phr TiC & 3 phr BN/epoxy	315.8 ± 0.4	42.8 ± 0.3	0.997
1 phr TiC & 5 phr BN/epoxy	313.1 ± 0.3	44.0 ± 0.2	0.998
3 phr TiC & 1 phr BN/epoxy	310.6 ± 0.4	39.5 ± 0.3	0.998
3 phr TiC & 3 phr BN/epoxy	309.4 ± 0.3	45.5 ± 0.3	0.998
3 phr TiC & 5 phr BN/epoxy	308.4 ± 0.5	48.2 ± 0.5	0.997
5 phr TiC & 1 phr BN/epoxy	302.5 ± 0.6	41.6 ± 0.5	0.997
5 phr TiC & 3 phr BN/epoxy	308.8 ± 0.5	41.6 ± 0.4	0.998
5 phr TiC & 5 phr BN/epoxy	312.6 ± 0.4	44.8 ± 0.3	0.998

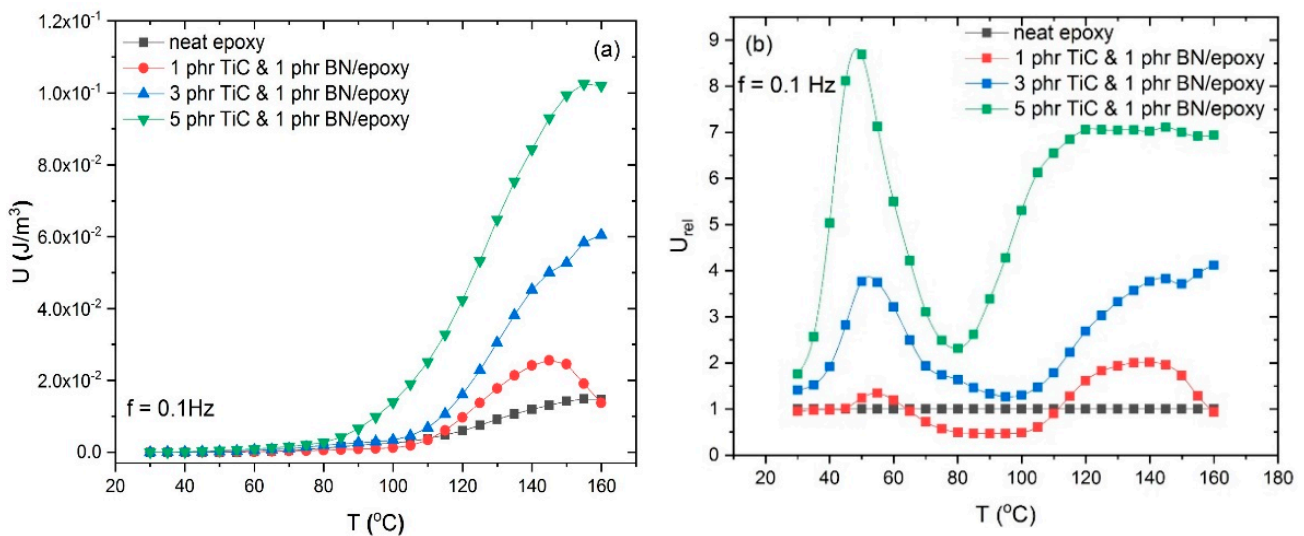


Figure 10. (a) Energy density as a function of temperature and (b) relative energy density, for the nanocomposites with 1 phr BN and varying TiC content, at 0.1 Hz.

In the vicinity of 50 °C, U_{rel} forms a peak (Figure 10b) associated with the glass–rubber transition. The increased segmental mobility of large parts of the macromolecular chains close to T_g enhances polarization and thus the ability to store energy, as expressed by the energy density. In this area, energy density appears to be almost nine times higher in the 5 phr TiC/1 phr BN/epoxy nanocomposite compared to the unfilled matrix. In addition, at relatively high temperatures optimum performance exhibits seven times higher energy storing ability for the same system than the unreinforced epoxy. In this area, IP is the dominating polarization mechanism.

The present study is focused on the dielectric response of the examined hybrid systems, which could induce a multifunctional performance. However, their potential application as electronic devices, portable (or even wearable) electronics, self-current regulators,

multilayer capacitors, conductive/semiconductive adhesives, electromagnetic radiation shielding, and energy storing media, should be accompanied by a suitable mechanical strength and durability. The mechanical behavior of the studied nanocomposites will be the subject of a forthcoming study. Representative mechanical properties of the employed matrix under static and dynamic conditions, at room temperature, are indicated by a Youngs' modulus higher than 1.5 GPa and a maximum storage modulus higher than 2.3 GPa [30,39]. Youngs' modulus, for nanocomposites produced via the same fabrication procedure, alerts to a value higher than 2.5 GPa for a system reinforced with 5 phr multi-wall carbon nanotubes, while maximum storage modulus exceeds 28.8 GPa for the 5 phr BN/epoxy nanocomposite.

5. Conclusions

In this work, hybrid TiC/BN/epoxy nanocomposites were fabricated with varying filler content. Morphological characterization conducted via SEM, and XRD confirmed that the specimens were successfully fabricated. Electrical properties were studied by means of BDS. Relaxation phenomena were evident in all dielectric graphs, implying the presence of relaxation processes such as interfacial polarization (IP), glass–rubber transition (α -process), and re-arrangement of polar side-groups (β -process), with ascending frequency, at constant temperature. Alternating conductivity varies exponentially with frequency at relatively high frequencies, while tends to its DC value in the low-frequency region. Values of the real part of dielectric permittivity appear to be dependent on the occurring interactions between polymer matrix and employed fillers, ϵ' increases with TiC content. Relaxation dynamics of α -process follows VFT relation. Finally, hybrid systems are capable of storing electrical energy as expressed by their energy density. The 5 phr TiC/1 phr BN/epoxy nanocomposite exhibits the highest energy density reaching at its maximum position nine times higher storing ability than the unfilled epoxy.

Author Contributions: For conceptualization, methodology, and validation, C.B., A.C.P. and G.C.P. are responsible; formal analysis, investigation, and data curation, was conducted by C.B., A.C.P. and G.C.P.; writing—original draft preparation, C.B.; writing—review and editing, A.C.P. and G.C.P.; supervision, and project administration, G.C.P. All authors have read and agreed to the published version of the manuscript.

Funding: This research received no external funding.

Data Availability Statement: Data are available upon request.

Acknowledgments: Authors would like to acknowledge Prof. N. Bouropoulos (Department of Materials Science, University of Patras and ICEHT-FORTH) for providing access to XRD facilities.

Conflicts of Interest: The authors declare no conflict of interest.

References

1. Song, K.; Guo, J.Z.; Liu, C. *Polymer-Based Multifunctional Nanocomposites and Their Applications*; Elsevier: Amsterdam, The Netherlands, 2019; ISBN 9780128150672.
2. Friedrich, K. Routes for achieving multifunctionality in reinforced polymers and composite structures. In *Multifunctionality of Polymer Composites*; Friedrich, K., Breuer, U., Eds.; Elsevier: Amsterdam, The Netherlands, 2015; pp. 3–41, ISBN 978-0-323-26434-1.
3. Chen, S.; Skordos, A.; Thakur, V. Functional nanocomposites for energy storage: Chemistry and new horizons. *Mater. Today Chem.* **2020**, *17*, 100304. [[CrossRef](#)]
4. Sanida, A.; Stavropoulos, S.G.; Speliotis, T.; Psarras, G.C. Evaluating the multifunctional performance of polymer matrix nanodielectrics incorporating magnetic nanoparticles: A comparative study. *Polymer* **2021**, *236*, 124311. [[CrossRef](#)]
5. Gioti, S.; Sanida, A.; Mathioudakis, G.N.; Patsidis, A.C.; Speliotis, T.; Psarras, G.C. Multitasking Performance of Fe₃O₄/BaTiO₃/Epoxy Resin Hybrid Nanocomposites. *Materials* **2022**, *15*, 1784. [[CrossRef](#)] [[PubMed](#)]
6. Dang, Z.-M.; Yuan, J.-K.; Yao, S.-H.; Liao, R.-J. Flexible Nanodielectric Materials with High Permittivity for Power Energy Storage. *Adv. Mater.* **2013**, *25*, 6334–6365. [[CrossRef](#)] [[PubMed](#)]
7. Thakur, V.K.; Gupta, R.K. Recent Progress on Ferroelectric Polymer-Based Nanocomposites for High Energy Density Capacitors: Synthesis, Dielectric Properties, and Future Aspects. *Chem. Rev.* **2016**, *116*, 4260–4317.

8. Manika, G.C.; Psarras, G.C. Barium titanate/epoxy resin composite nanodielectrics as compact capacitive energy storing systems. *Express Polym. Lett.* **2019**, *13*, 749–758. [[CrossRef](#)]
9. Psarras, G.C. Nanodielectrics: An emerging sector of polymer nanocomposites. *Express Polym. Lett.* **2008**, *2*, 460. [[CrossRef](#)]
10. Gibson, G. *Epoxy Resins, Brydson's Plastics Materials*; Elsevier: Amsterdam, The Netherlands, 2017; pp. 773–797.
11. Patsidis, A.C.; Psarras, G.C. Dielectric and Conductivity Studies of Epoxy Composites. In *Epoxy Composites: Fabrication, Characterization and Applications*, 1st ed.; Parameswaranpillai, J., Pulikkalparambil, H., Rangappa, S.M., Siengchin, S., Eds.; WILEY-VCH GmbH: Weinheim, Germany, 2021; pp. 299–348, ISBN 9783527824083.
12. Wang, J.; Ma, F.; Sun, M. Graphene, hexagonal boron nitride, and their heterostructures: Properties and applications. *RSC Adv.* **2017**, *7*, 16801–16822. [[CrossRef](#)]
13. Chang, H.; Wu, H. Graphene-based nanocomposites: Preparation, functionalization, and energy and environmental applications. *Energy Environ. Sci.* **2013**, *6*, 3483–3507. [[CrossRef](#)]
14. Raptis, C.G.; Patsidis, A.; Psarras, G.C. Electrical response and functionality of polymer matrix-titanium carbide composites. *Express Polym. Lett.* **2010**, *4*, 234–243. [[CrossRef](#)]
15. Liu, Y.; Oshima, K.; Yamauchi, T.; Shimomura, M.; Miyauchi, S. Temperature-conductivity characteristics of the composites consisting of fractionated poly(3-hexylthiophene) and conducting particles. *J. Appl. Polym. Sci.* **2000**, *77*, 3069–3076. [[CrossRef](#)]
16. Sung, Y.K.; El-Tantawy, F. Novel smart polymeric composites for thermistors and electromagnetic wave shielding effectiveness from TiC loaded styrene-butadiene rubber. *Macromol. Res.* **2002**, *10*, 345–358. [[CrossRef](#)]
17. El-Tantawy, F. New double negative and positive temperature coefficients of conductive epdm rubber TiC ceramic composites. *Eur. Polym. J.* **2002**, *38*, 567–577. [[CrossRef](#)]
18. Wang, F.; Zhou, D.; Gong, S. Dielectric behavior of TiC-PVDF nanocomposites. *Phys. Status Solid Rapid Res. Lett.* **2009**, *3*, 22–24. [[CrossRef](#)]
19. Cui, M.; Ren, S.; Qin, S.; Xue, Q.; Zhao, H.; Wang, L. Non-covalent functionalized hexagonal boron nitride nanoplatelets to improve corrosion and wear resistance of epoxy coatings. *RSC Adv.* **2017**, *7*, 44043–44053. [[CrossRef](#)]
20. Chen, T.M.; Xiao, J.; Yang, G.W. Cubic boron nitride with an intrinsic peroxidase-like activity. *RSC Adv.* **2016**, *6*, 70124. [[CrossRef](#)]
21. Swanson, H.E.; McMurdie, H.F.; Morris, M.C.; Evans, E.H. *Standard X-ray Diffraction Powder Patterns: NBS Monograph 25—Section 5*; National Bureau of Standards Reports; Government Printing Office: Gaithersburg, MD, USA; Washington, DC, USA, 1967.
22. Psarras, G.C. Conductivity and dielectric characterization of polymer nanocomposites. In *Physical Properties and Applications of Polymer Nanocomposites*; Tjong, S.C., Mai, Y.-W., Eds.; Woodhead Publishing: Cambridge, MA, USA, 2010; pp. 31–69, ISBN 9781845696726.
23. Kalini, A.; Gatos, K.G.; Karahaliou, P.K.; Georga, S.N.; Krontiras, C.A.; Psarras, G.C. Probing the Dielectric Response of Polyurethane/Alumina Nanocomposites. *J. Polym. Sci. Part B Polym. Phys.* **2010**, *48*, 2346–2354. [[CrossRef](#)]
24. Vryonis, O.; Anastassopoulos, D.L.; Vradis, A.A.; Psarras, G.C. Dielectric response and molecular dynamics in epoxy-BaSrTiO₃ nanocomposites: Effect of nanofiller loading. *Polymer* **2016**, *95*, 82–90. [[CrossRef](#)]
25. Steeman, P.A.M.; van Turnhout, J. Dielectric properties of inhomogeneous media. In *Broadband Dielectric Spectroscopy*; Kremer, F., Schönhals, A., Eds.; Springer: Berlin, Germany, 2003; pp. 495–522. ISBN 3-540-43407-0.
26. Jonscher, A.K. *Universal Relaxation Law*; Chelsea Dielectrics Press: London, UK, 1992; Chapter 5.
27. Dyre, J.C.; Schröder, T.B. Hopping models and ac universality. *Phys. Stat. Sol. B* **2002**, *230*, 5–13. [[CrossRef](#)]
28. Psarras, G.C. Hopping conductivity in polymer matrix–metal particles composites. *Compos. Part A Appl. Sci. Manuf.* **2006**, *37*, 1545–1553. [[CrossRef](#)]
29. Tsangaris, G.M.; Psarras, G.C.; Manolakaki, E. DC and AC conductivity in polymeric particulate composites. *Adv. Comp. Letts.* **1999**, *8*, 25–29.
30. Konstantinou, A.C.; Patsidis, A.C.; Psarras, G.C. Boron nitride/epoxy resin nanocomposites: Development, characterization and functionality. *J. Therm. Anal. Calorim.* **2021**, *145*, 2925–2933. [[CrossRef](#)]
31. Tsangaris, G.M.; Psarras, G.C.; Kouloumbi, N. Electric modulus and interfacial polarization in composite polymeric systems. *J. Mater. Sci.* **1998**, *33*, 2027–2037. [[CrossRef](#)]
32. Hernández, M.; Carretero-González, J.; Verdejo, R.; Ezquerro, T.A.; López-Manchado, M.A. Molecular dynamics of natural rubber/layered silicate nanocomposites as studied by dielectric relaxation spectroscopy. *Macromolecules* **2010**, *43*, 643–651. [[CrossRef](#)]
33. Belattar, J.; Achour, M.E.; Brosseau, C. A comparison between the permittivity and electric modulus representations of the microwave response of carbon black loaded polymer composites under uniaxial tension. *J. Appl. Phys.* **2011**, *110*, 054101. [[CrossRef](#)]
34. Koufakis, E.; Mathioudakis, G.N.; Patsidis, A.C.; Psarras, G.C. ZnTiO₃/epoxy resin nanocomposites: Development, dielectric behaviour and functionality. *Polym. Test.* **2019**, *77*, 105870. [[CrossRef](#)]
35. Peng, X.; Liu, X.; Qu, P.; Yang, B. Enhanced breakdown strength and energy density of PVDF composites by introducing boron nitride nanosheets. *J. Mater. Sci. Mater. Electron.* **2018**, *29*, 16799–16804. [[CrossRef](#)]
36. Mijović, J.; Lee, H.K.; Kenny, J.; Mays, J. Dynamics in polymer-silicate nanocomposites as studied by dielectric relaxation spectroscopy and dynamic mechanical spectroscopy. *Macromolecules* **2006**, *39*, 2172–2182. [[CrossRef](#)]
37. Sanida, A.; Stavropoulos, S.G.; Speliotis, T.; Psarras, G.C. Development, characterization, energy storage and interface dielectric properties in SrFe₁₂O₁₉/epoxy nanocomposites. *Polymer* **2017**, *120*, 73–81. [[CrossRef](#)]

38. Drakopoulos, S.X.; Patsidis, A.C.; Psarras, G.C. Epoxy-based/BaTiO₃ nanodielectrics: Relaxation dynamics, charge transport and energy storage. *Mater. Res. Bull.* **2022**, *145*, 111537. [[CrossRef](#)]
39. Stavropoulos, S.G.; Sanida, A.; Psarras, G.C. Assessing the effect of Fe₃O₄ nanoparticles on the thermomechanical performance of different forms of carbon allotropes/epoxy hybrid nanocomposites. *Appl. Mech.* **2022**, *3*, 560–572. [[CrossRef](#)]